

Sequence-Selective Organoiridium DNA Bis-Intercalators with Flexible Dithiaalkane Linker Chains

Malte Kokoschka,^[a] Jan-Amadé Bangert,^[a] Raphael Stoll,^[a] and William S. Sheldrick^{*[a]}

Keywords: DNA / DNA recognition / Iridium / Intercalation / Polypyridyl ligands

The rapid DNA intercalation by dinuclear polypyridyl (η^5 -C₅Me₅)Ir^{III} complexes of the type $[(\eta^5\text{-C}_5\text{Me}_5)\text{Ir}(\text{dppz})]_2(\mu\text{-L})(\text{CF}_3\text{SO}_3)_4$ **1–4** has been studied by UV/Vis spectroscopy, circular dichroism, viscosity measurements and nuclear magnetic resonance. Whereas the Ir atoms of compounds **1–3** are linked by flexible dithiaalkanes of the type L = CH₂S(CH₂)_n-SCH₃ (*n* = 4–6), compound **4** contains cyclic 1,4-dithiane as a shorter more rigid bridging ligand. Stable intercalative binding into CT DNA is indicated for **1–3** by large increases

in the DNA thermal denaturation temperature and by induced negative CD bands at about 300 nm. Viscosity measurements show that the DNA lengthening induced by the bis-intercalators **1–3** is about twice that caused by the monointercalator **4**. An analysis of the NOE cross-peaks for a 1:1 mixture of **3** with the double-strand decanucleotide d(5'-GCGCATCGGC-3') demonstrates that **3** intercalates in a sequence-specific manner from the minor groove between the base pairs C4–G17 and A5–T16, and T6–A15 and C7–G14.

Introduction

Octahedral ruthenium(II) and rhodium(III) complexes containing large polypyridyl ligands such as dipyrro[2,3-*a*:2',3'-*c*]phenazine (dppz) have received considerable recent attention owing to their ability to target specific DNA base sequences through intercalative binding.^[1–4] In analogy to organic intercalators such as the anthraquinone doxorubicin, which is in clinical use for the treatment of a wide range of human cancers,^[3] metalointercalators might also be expected to exhibit potential as anticancer agents.^[5] However, octahedral metalointercalators containing two or three polypyridyl ligands have not shown particular promise as anticancer agents although [RhCl₂(dppz)(phen)]Cl does exhibit appreciable cell toxicity towards human tumour cells following irradiation at 311 nm.^[6]

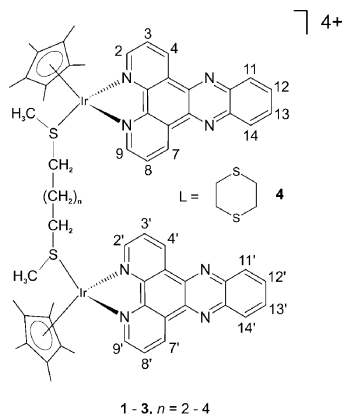
In contrast, we have recently reported significant cytotoxicity for members of the organometallic series $[(\eta^6\text{-C}_6\text{Me}_6)\text{RuCl}(\text{pp})]^+$, $[(\eta^5\text{-C}_5\text{Me}_5)\text{RhCl}(\text{pp})]^+$ and $[(\eta^5\text{-C}_5\text{Me}_5)\text{IrCl}(\text{pp})]^+$ (pp = dpq, dppz, dppn; dpq = dipyrro[3,2-*d*:2',3'-*f*]quinoxaline; dppn = benzo[*i*]dipyrro[3,2-*a*:2',3'-*c*]phenazine) containing just one polypyridyl ligand.^[7–9] Their IC₅₀ values towards human MCF-7 (breast cancer) and HT-29 cells (colon cancer) lie in the range 30.3–0.13 μM and correlate with the size of the polypyridyl ligand, i.e. decreasing IC₅₀ values are observed in the order dpq > dppz > dppn. Effective intercalation into DNA has been established by UV/Vis and NOESY spectroscopy for

analogous half-sandwich complexes of the types $[(\eta^6\text{-C}_6\text{Me}_6)\text{Ru}(\text{dppz})(\text{L})]^{2+}$ and $[(\eta^5\text{-C}_5\text{Me}_5)\text{Ir}(\text{dppz})(\text{L})]^{2+}$ incorporating methionine-containing amino acids and peptides L.^[10,11] In view of recent attempts to enhance the cytotoxicity and DNA specificity of metalointercalators by combining the intercalating fragment with a second functionality,^[3] it is attractive to connect two $\{(\eta^6\text{-C}_6\text{Me}_6)\text{-Ru}(\text{dppz})\}^{2+}$ or $\{(\eta^5\text{-C}_5\text{Me}_5)\text{Ir}(\text{dppz})\}^{2+}$ fragments into a potential bis-intercalator through a linking chain. A first example of this type of complex was provided by $[(\eta^5\text{-C}_5\text{Me}_5)\text{Ir}(\text{dppz})]_2(\mu\text{-L})^{5+}$ (L = H₂-Met-Met-OH, H-Met-OH = L-methionine), which turned out, however, to be a monointercalator, presumably owing to the lack of conformational flexibility of its peptide backbone.^[12] It is interesting to note, that the dinuclear complexes $\{[(\text{CO})_3\text{Re}(\text{dppz})]_2(\mu\text{-L})\}^{2+}$ (L = 1,2-bis(4-pyridyl)ethane and 1,2-bis(4-pyridyl)propane),^[13] $\{[(\text{tpm})\text{Ru}(\text{dppz})]_2(\mu\text{-dpp})\}^{4+}$ and $\{[(\text{CO})_3\text{Re}(\text{dppz})](\mu\text{-dpp})\{(\text{tpm})\text{Ru}(\text{dppz})\}\}^{3+}$ [dpp = 1,2-bis(4-pyridyl)pentane, tpm = tris(1-pyrazolyl)methane]^[14,15] are also monointercalators despite the apparent flexibility of their linking polymethylene chains. In contrast, Nordén et al. have been successful in designing an octahedral ruthenium(II) bis-intercalator $\{[(\text{phen})_2\text{Ru}]\{(\mu\text{-C}_4(\text{cpdppz})_2)\}^{4+}$, in whose bridging C₄(cpdppz)₂ ligand two dppz moieties are connected by an aliphatic diamide linker.^[16,17] Following initial formation of a groove-bound adduct, slow rearrangement leads to intrastrand bis-intercalation involving the threading of one of the $\{(\text{phen})_2\text{Ru}\}^{2+}$ fragments through the DNA duplex.

These findings prompted us to investigate the suitability of more flexible 2,*n*-dithiaalkane ligands (*n* = 7, 8, 9) for enabling rapid sequence-selective bis-intercalation of dinuclear $\{(\eta^5\text{-C}_5\text{Me}_5)\text{Ir}(\text{dppz})\}^{2+}$ complexes of the type

[a] Fakultät für Chemie und Biochemie, Ruhr-Universität Bochum, 44780 Bochum, Germany
Fax: +49-234-3214420
E-mail: william.sheldrick@rub.de

$[(\eta^5\text{-C}_5\text{Me}_5)\text{Ir}(\text{dppz})_2(\mu\text{-L})](\text{CF}_3\text{SO}_3)_4$ **1–3** with $\text{L} = 2,7$ -dithiaoctane, 2,8-dithianonane and 2,9-dithiadecane (Scheme 1). An analogous diiridium(III) complex **4** (Scheme 1) with the less flexible cyclic 1,4-dithiane ligand was studied for comparison purposes.



Scheme 1. Cations of the compounds $[(\eta^5\text{-C}_5\text{Me}_5)\text{Ir}(\text{dppz})_2(\mu\text{-L})](\text{CF}_3\text{SO}_3)_4$ **1–4**.

Results and Discussion

Synthesis and Structures of **1–4**

The dinuclear complexes of the type $[(\eta^5\text{-C}_5\text{Me}_5)\text{Ir}(\text{dppz})_2(\mu\text{-L})](\text{CF}_3\text{SO}_3)_4$ **1–4** were prepared by refluxing the solvent complex $[(\eta^5\text{-C}_5\text{Me}_5)\text{Ir}(\text{acetone})(\text{dppz})](\text{CF}_3\text{SO}_3)_2$ with the appropriate dithiaalkane bridging ligand in $\text{CH}_3\text{OH}/\text{CH}_2\text{Cl}_2$ at a 2:1 molar ratio for 48 h. Compounds **1–4** were characterised by ^1H NMR spectroscopy and positive-ion LSIMS and gave satisfactory microanalyses. The structure of **4** was determined by X-ray structural analysis. As depicted in Figures 1 and 2, the triclinic unit cell of **4** contains two contrasting rotamers of the dinuclear tetracation at a 1:2 ratio in addition to eight water molecules of crystallisation. Crystallographic C_i symmetry is observed for the first of the rotamers (Figure 1), which means that it adopts a *trans* arrangement of its polypyridyl ligands. In contrast, the dppz ligands are twisted towards one another about the central $\text{Ir}\cdots\text{Ir}'$ axis in the second rotamer, whose $(\text{dppz})\text{-Ir}\cdots\text{Ir}'\text{-(dppz')}$ torsion angle of 114° is close to that of 120° expected for a *gauche*(–) conformation (Figure 2). The $\text{Ir}\cdots\text{Ir}'$ distance of 7.69 \AA is somewhat shorter than that of 7.84 \AA in the first rotamer. Inspection of Figure 1 and 2 indicates that the energetically favourable chair conformation is adopted by the 1,4-dithiane ligand in both cases and that the $\{(\eta^5\text{-C}_5\text{Me}_5)\text{Ir}(\text{dppz})\}^{2+}$ fragments are sited equatorially relative to the six-membered rings. Free rotation about the individual Ir-S bonds will be restricted by potential intramolecular contacts between protons of the $[\text{C}_5\text{Me}_5]^-$ and 1,4-dithiane ligands.

Although conformational flexibility is to be expected for the bridging 2,*n*-dithiaalkane ligands of complexes **1–3**, their ^1H NMR spectra in CD_3OD are in accordance with the presence of 4 competing solution species in each case.

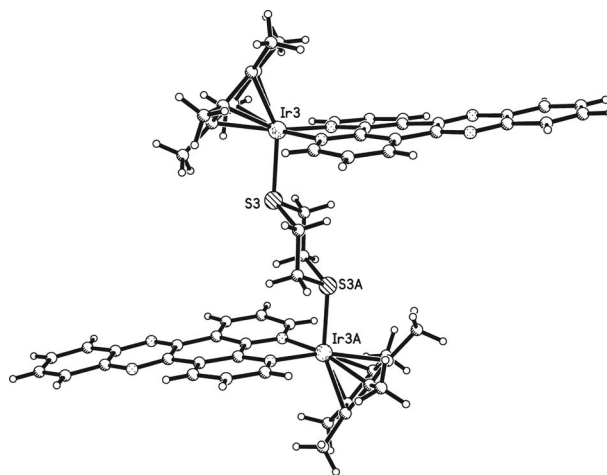


Figure 1. Molecular structure of the *trans* rotamer of **4**.

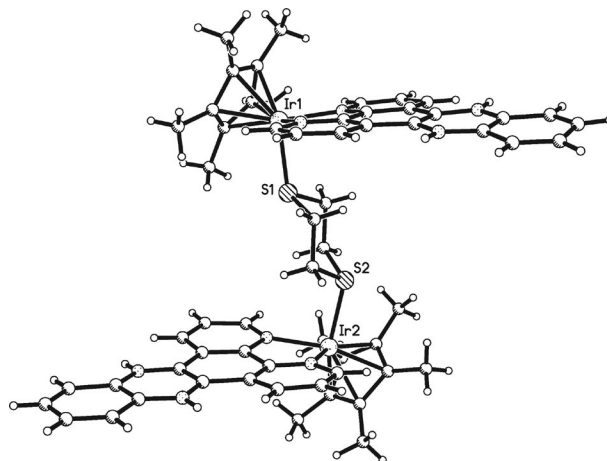


Figure 2. Molecular structure of the *gauche*(–) rotamer of **4**.

As illustrated in Figure 3 (a) for the aromatic region of the 2,8-dithiadecane complex **3**, four distinct doublets with differing integral intensities are observed for the low field 2/9 and 4/7 proton signals of the dppz ligands of the dinuclear tetracation. Dilution to a concentration of one tenth of the original concentration leads to an increase in the integral values for the signals of highest and third highest intensity relative to the other two signals for the individual protons. This suggests that the former resonances may belong to monomeric species and the latter to dimeric and/or oligomeric species that could result from intermolecular $\pi\text{-}\pi$ stacking interactions between the extended aromatic surfaces of the planar dppz ligands.

It is instructive to compare the ^1H NMR spectra of complexes **1–3** with that of the 1,4-dithiane complex **4** (Figure 3, b) for which fewer solution species might be predicted owing to the restricted rotation about the central $\text{Ir}\cdots\text{Ir}'$ axis. In this case, four doublets are once again observed for the dppz 2/9 and 4/7 protons, respectively, of which one pair is of very low integral intensity and two other pairs exhibit identical integral intensities. As the 2/9 and 4/7 protons will be magnetically equivalent in the *trans* rotamer of Figure 1

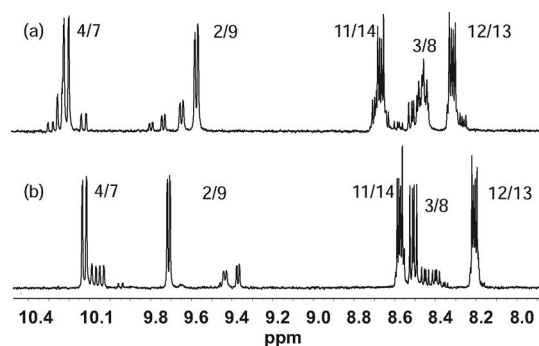


Figure 3. ^1H NMR spectrum of the aromatic region of (a) the $[(\eta^5\text{-C}_5\text{Me}_5)\text{Ir}(\text{dppz})_2(\mu\text{-1,8-dithiadecane})]^{4+}$ cation of **3**, and (b) $[(\eta^5\text{-C}_5\text{Me}_5)\text{Ir}(\text{dppz})_2(\mu\text{-1,4-dithiane})]^{4+}$ cation of **4**, both in CD_3OD solution.

but non-equivalent in the *gauche*(–) rotamer of Figure 2, it is possible that the solid-state rotamers may also dominate in CD_3OD solution, albeit at an effectively reversed integral ratio of 0.68:0.32.

DNA Binding Studies

Whereas a lengthening of 3.4 Å per intercalated aromatic moiety is predicted for the DNA double helix in the classical intercalation model, electric dichroism measurements have suggested a range of possible helix extensions, from 2.0 to 3.7 Å, depending on the nature of the intercalating compound.^[18] As a result of intercalation, the usual rotation of approximately 36° for neighbouring base-pairs is restricted to about 26°.^[19,20] With few exceptions, it is generally accepted that the presence of an intercalator between two base-pairs will exclude the nearest neighbouring sites from being occupied by another intercalator. This nearest neighbour exclusion principle^[21] stipulates that the intercalating moieties in an intrastrand bis-intercalator must sandwich a minimum of two base-pairs, which corresponds to a distance of about 10.2 Å (3×3.4 Å intercalation sites). Force field calculations with the Hyperchem package^[22] indicate that the relative conformational energy of the 1,7-dithiaoctane ligand increases rapidly for Ir···Ir' distances above about 8 Å, whereas the longer 1,8-dithianonane and 1,9-dithiadecane ligands can support intermetal distances of up to respectively 11.5 and 13 Å with energetically favourable polyalkane conformations. This suggests that complexes **2** and **3** should be potentially capable of functioning as intrastrand bis-intercalators by sandwiching two base pairs. Complex **1** could also be a candidate for this type of binding mode by sandwiching just one base pair at a dppz···dppz distance of about 6.8 Å, but this would contradict the nearest neighbour exclusion principle.

Following incubation periods of 2 min, UV/Vis spectra of buffered solutions of the complexes **1–4** (10 mM phosphate buffer, pH 7.2) with CT DNA at 25 °C and a [complex]/[DNA] ratio of $r = 0.1$ {[DNA] gives the DNA concentration as M(base pairs)} exhibit no further significant changes over a period of 48 h. This indicates that achieve-

ment of equilibrium conditions must be rapid in each case. Pronounced decreases in absorbance for complexes **1–4** at about 364 and 385 nm and bathochromic shifts in the range 5–7 nm for these absorption maxima are indicative of dppz intercalation into the DNA double helix in all cases. The hypochromic shift $\Delta A/A$ of –47.6% at 385 nm with its associated red shift of 5 nm is depicted for complex **3** in Figure 4. A steady increase in $-\Delta A/A$ is observed on going from **1** (–30.5%) to complex **2** (–36.7%) and then **3** (–47.6%), which suggests that there may be a direct correlation between the effectiveness of dppz intercalation and the chain length of the 2,*n*-dithiaalkane bridging ligand. The hypochromic shifts $\Delta A/A$ for complexes **2** and **3** at $r = 0.1$ are similar to that of –44% for $[(\eta^5\text{-C}_5\text{Me}_5)\text{Ir}(\text{dppz})\{(\text{NMe}_2)_2\text{-CS}\}](\text{CF}_3\text{SO}_3)_2$ at $r = 0.2$,^[7] i.e. with the same molar ratio of dppz ligands to DNA base pairs. Although this observation is clearly in accordance with the participation of both of the dppz ligands of **2** and **3** in DNA intercalation, it is not possible to draw any definite conclusions from these findings. This is because a value of –43.2% is observed for $\Delta A/A$ at 385 nm in the case of the 1,4-dithiane complex **4**, for which intrastrand bis-intercalation will be clearly sterically unfavourable.

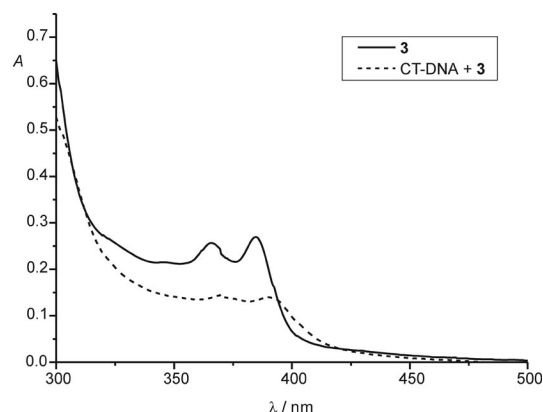


Figure 4. UV/Vis spectra of complex **3** (10 μM) and its equilibrium mixture with CT DNA (100 μM) in a 10 mM phosphate buffer (pH 7.2) at $r = 0.1$ after 2 min.

Thermal denaturation measurements for CT DNA in the presence of transition metal complexes such as **1–4** can also provide a means of gauging the strength of dppz intercalation, provided that electrostatic and hydrogen bonding interactions remain effectively unchanged by variation of the bridging ligand.^[12,23] The ΔT_m values (Table 1) were recorded under equilibrium conditions in a 10 mM phosphate buffer at pH 7.2 for 1:20 complex/DNA mixtures and are indicative of very strong DNA interactions for complexes **1–3**. Values of 5.8–7.8 °C have been previously reported for compounds of the type $[(\eta^5\text{-C}_5\text{Me}_5)\text{Ir}(\text{dppz})(\text{L})]^{n+}$, $n = 2, 3$, containing methionine-containing amino acids and peptides,^[11] and of respectively 15.2 and 11.2 °C for the more highly charged monointercalating dinuclear complexes $[(\eta^5\text{-C}_5\text{Me}_5)\text{Ir}]_2(\mu\text{-H}_2\text{-Met-Met-OH})^{5+}$ and $[(\eta^5\text{-C}_5\text{Me}_5)\text{Ir}](\mu\text{-H-Gly-Met-OH-}\kappa\text{S};\kappa\text{N}_G)\{\text{Pt}(\text{tpy})\}^{4+}$ (H-Gly-OH = glycine, tpy = 2,2':6',2''-terpyridine).^[12] However, these

measurements were performed at a four times higher 1:5 complex/DNA ratio. As the melting temperatures for T_m mixtures of **1–3** with CT DNA at this molar ratio were found to lie above the experimentally accessible range (67–85 °C) for a 10 mM phosphate buffer, the lower 1:20 molar ratio ($r = 0.05$) was chosen so as to enable a ΔT_m comparison within the reliable 0–15 °C range. The observed ΔT_m values increase from 6.3 for **1** over 7.2 for **2** up to 9.3 °C for complex **3**. In contrast, a much lower value of 3.3 °C was observed for the 1,4-dithiane complex **4** at the same molar ratio. These findings are once again in accordance with an increase in binding efficacy in the order of increasing chain length of the bridging ligand and suggest that complexes **2** and **3** may indeed function as effective bis-intercalators.

Table 1. ΔT_m and $(L - L_0)/(L_0 \cdot r)$ values for CT DNA in the presence of complexes **1–4**.

Complex	Bridging ligand	ΔT_m [°C] ^[a]	$(L - L_0)/(L_0 \cdot r)$ ^[b]
1	2,7-dithiaoctane	6.3	1.01
2	2,8-dithianonane	7.2	1.03
3	2,9-dithiadecane	9.3	1.06
4	1,4-dithiane	3.3	0.52

[a] For complex/DNA mixtures at $r = 0.05$ in a 10 mM phosphate buffer. [b] Based on $(\eta/\eta_0)^{1/3} = (L/L_0)$ values for reduced viscosity measurements on DNA alone (η_0) and complex/DNA mixtures (η) at $r = 0.1$; L_0 = length of DNA alone and L = length of DNA at $r = 0.1$.

Characteristic changes in the observed circular dichroism (CD) spectra of DNA in the range 220–350 nm provide a convenient means of monitoring conformational changes for the biopolymer.^[24–26] It has previously been established that the appearance of a characteristic negative ICD band at about 300 nm is indicative of dppz intercalation into the double helix.^[7,8,23]

Both complexes **2** and **3** (Figure 5) exhibit pronounced negative ICD bands at about 298 nm with respective molar ellipticities $[\theta]$ of -2.43 and $-2.56 \text{ deg cm}^2 \text{ dmol}^{-1} \times 10^{-3}$ for complex/DNA molar ratios of 1:10. In contrast much lower $[\theta]$ values of -0.91 and -0.56 were observed for the 2,8-dithiaoctane and 1,4-dithiane complexes **1** and **4**. The significant blue shifts of respectively 6 and 3 nm for the positive CT DNA band of the mixtures **2**/DNA and **3**/DNA are also in accordance with stable dppz intercalation.^[23] Hypsochromic shifts of 2 and 5 nm were recorded for **1** and **4**, respectively.

Convincing evidence for DNA intercalation can often be obtained from viscosity measurements.^[27,28] Insertion of aromatic ligands between adjacent nucleobase pairs causes a lengthening and stiffening of the double helix and these changes are reflected in an increase in DNA viscosity. The reduced viscosity function $(\eta/\eta_0)^{1/3}$ is equal to (L/L_0) , where η and L are the reduced viscosity and length of the intercalated DNA at a given complex/DNA ratio r , and η_0 and L_0 are the corresponding values for DNA alone.^[27] At low complex/DNA ratios in the range $0 \leq r \leq 0.1$, ideal mono-intercalation or bis-intercalation should lead to expected values of respectively 1.0 and 2.0 for the function $(L - L_0)/$

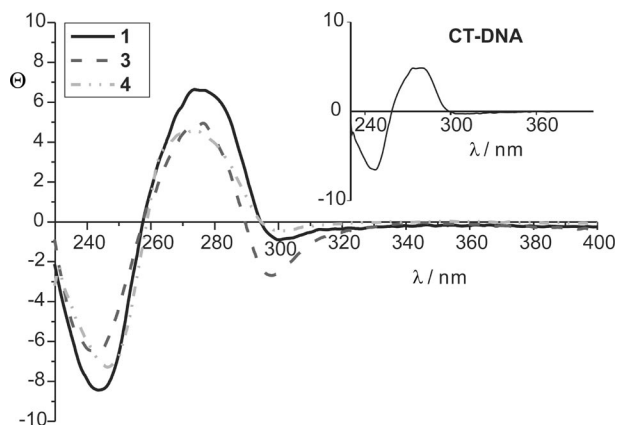


Figure 5. CD spectra of CT DNA and mixtures of complexes **1**, **3** and **4** with CT DNA in a 10 mM phosphate buffer (pH 7.2) at $r = 0.1$ after 24 h incubation.

$(L_0 \cdot r)$. These values reflect the classical model of intercalation, where the helix is lengthened by 3.4 Å per intercalated moiety. In fact, a much wider range of helix extensions from 2.0 to about 3.7 Å has been established for aromatic molecules by electric dichroism measurements^[18] and relatively low increases in DNA length are often recorded in the presence of metallointercalators. The observed $(L - L_0)/(L_0 \cdot r)$ value of 0.52 for a complex **4**/DNA mixture at $r = 0.1$ is very similar to that of 0.53 obtained for the mono-intercalator $[(\eta^6\text{-C}_6\text{Me}_6)\text{RuCl}(\text{dppz})](\text{CF}_3\text{SO}_3)$.^[8] Such values indicate that dppz intercalation by bulky organometallic half-sandwich complexes may well be associated with a marked degree of duplex distortion. $(L - L_0)/(L_0 \cdot r)$ values in the range 1.01–1.06 (Table 1) are in accordance with an approximate doubling of the DNA lengthening in the presence of the flexible 2, n -dithiaalkane complexes **1–3**, when compared with the complex **4**/DNA mixture. Taken together with the significantly higher ΔT_m values, they are clearly indicative of a bis-intercalating binding mode for **1–3**.

NOESY Studies

Both intra- or intermolecular bis-intercalation could be possible for complexes **1–3**. Conclusive evidence for the former DNA binding mode was obtained for complex **3** from an NMR spectroscopic study of its interaction with the double-strand decanucleotide d(5'-GCGCATCGGC-3') (Figure 6).

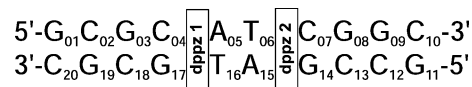


Figure 6. The numbering scheme and bis-intercalation site of complex **3** for its binding interaction with the double-strand decanucleotide d(5'-GCGCATCGGC-3').

Addition of **3** to the decanucleotide at a 1:1 molar ratio at 293 K induces significant upfield chemical shift changes of -0.22 , -0.19 and -0.32 ppm for the G3–H8, T6–H6 and

C13–H6 protons, respectively (Table 2). In contrast, A15–H8 and G17–H8 experience opposite downfield shifts of 0.24 and 0.31 (Figure 7, b). Of particular note are the pronounced upfield shifts of 0.30 and 0.20 ppm recorded for the T6 and T16 methyl resonances, respectively. The dppz protons also experience large upfield shifts on metal complex binding to the decanucleotide in phosphate-buffered saline (PBS) in comparison to the values for the metal complex itself in CD₃OD. For instance, upfield changes in the range 0.4–0.7 and 1.1–1.6 ppm are observed for the H2/H9 and H4/H7 protons, respectively. Such dramatic increases in shielding are clearly consistent with dppz intercalation,^[29,30] as is the concomitant broadening of the resonances on addition of the metal complex to the decanucleotide.

Table 2. ¹H NMR chemical shifts (ppm) of the nucleobase protons in d(5'-GCGCATCGGC-3') and the chemical shift differences (in parentheses) induced by addition of complex **3** at a molar 1:1 ratio in phosphate-buffered saline containing 20 mM NaCl at pH 7.2 and 298 K.

Base	H6/H8	Base	H6/H8
G1	7.92 (–0.04)	C20	7.44 (–0.06)
C2	7.37 (–0.10)	G19	7.87 (–0.08)
G3	7.86 (–0.22)	C18	7.27 (–0.08)
C4	7.31 (–0.08)	G17	7.70 (0.31)
A5	8.25 (0.09)	T16	7.00 (–0.01)
T6	7.13 (–0.19)	A15	8.14 (0.24)
C7	7.35 (0.14)	G14	7.88 (–0.08)
G8	7.83 (–0.15)	C13	7.40 (–0.32)
G9	7.72 (–0.05)	C12	7.47 (–0.08)
C10	7.40 (–0.04)	G11	7.95 (–0.04)

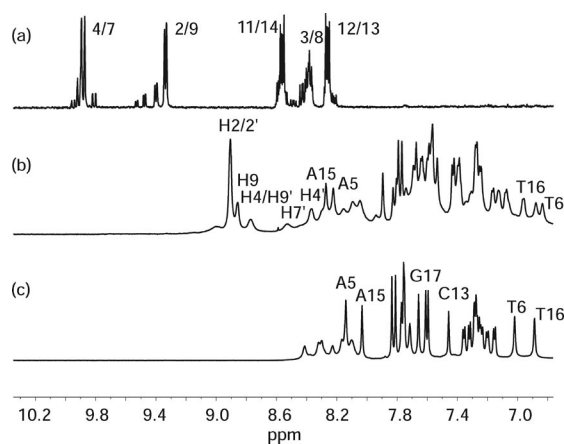


Figure 7. 1D ¹H NMR spectra of (a) complex **3** in CD₃OD, (b) complex **3** bound to the decanucleotide d(5'-GCGCATCGGC-3') at a molar ratio of 1:1 and (c) the free decanucleotide both in phosphate-buffered saline (PBS) containing 20 mM NaCl at pH 7.2 and 293 K.

The intraduplex NOE cross peaks of the type n H1' → ($n+1$) H6/8 are interrupted for the nucleotide sequences C4/A5, T6/C7, C7/G8, C13/G14 and T16/G17 in the 100 ms NOESY spectrum of the 1:1 mixture of complex **3** and d(5'-GCGCATCGGC-3'). This observation is indicative of metal complex binding causing large increases in the intramolecular distances between the relevant decanucleotide

bases. In addition to the expected sequential NOEs for the other base pairs, the NOESY spectrum also contains a number of intermolecular cross peaks between the protons of the dppz ligands and the duplex nucleotides (Table 3). Of particular note are the NOEs (Figure 8, b) from the H4, H7/H8 and H9 protons of one dppz ligand to the minor groove T6–H1', G14–H1' and A15–H1' sugar protons, respectively. These contacts are in accordance with dppz intercalation between the T6–A15 and C7–G14 base pairs in the decanucleotide minor groove. Consistent with this proposal are also the medium-strength NOEs between the dppz protons H11/12/13 and the T6 methyl group (Figure 8, a), which protrudes into the major groove. Although fewer NOE cross peaks are observed for the second dppz ligand, the large upfield shifts experienced by its H2'/9' and H4'/H7' protons and the presence of NOEs (Figure 8, b) from H2', H4' and H7' to G17–H1', T16–H1' and C4–H1', respectively, are once again indicative of minor groove intercalation, in this case between the C4–G17 and A5–T16 base pairs. Further evidence for this binding mode is provided by the NOE cross peaks between H11'–H13' and the methyl protons of T16. Taken together with the interruption of the sequential n H1' → ($n+1$) H6/8 contacts for $n = 4, 6$ and 16, the observed pattern of intermolecular NOEs indicates that the intercalating dppz ligands sandwich the base pairs A5–

Table 3. Intermolecular NOE cross peaks (ppm) observed between the dppz protons of complex **3** and the nucleotide protons of d(5'-GCGCATCGGC-3') at a metal complex/duplex ratio of 1:1 in phosphate-buffered saline containing 20 mM NaCl at pH 7.2 and 298 K.

dppz H [δ]	Oligonucleotide H [δ] ^[a]			
Ligand 1	T6	C7	A15	G14
H2	9.02	H3' 5.10 (w)		
H4	8.88	H2' 2.36 (m) H2'' 2.45 (m) H1' 5.64 (m) H6 6.95 (w)		
H7	8.35			H1' 5.50 (s)
H8	7.60			H1' 5.50 (w)
H9	8.97		H5' 4.40 (w) H4' 4.51 (m) H1' 5.49 (w)	
H11	7.53	CH ₃ 1.04 (m) H2' 2.36 (m) H2'' 2.45 (m) H6 6.95 (m)	H5' 5.72 (m)	H1 12.08 (m)
H12	7.70	CH ₃ 1.04 (m) H6 6.95 (w)	H5' 5.72 (m)	
H13	7.75	CH ₃ 1.04 (m)		
H14	7.50	CH ₃ 1.04 (w)		
Ligand 2	C4	A5	G17	T16
H2'	9.02		H1' 5.64 (m)	
H4'	8.48			H2' 2.20 (m) H2'' 2.35 (m) H1' 5.60 (m)
H7'	8.64	H1' 5.45 (m)		
H11'	7.53			CH ₃ 1.13 (m)
H12'	7.70			CH ₃ 1.13 (m)
H13'	7.74			CH ₃ 1.13 (w)

[a] s = strong, m = medium, w = weak.

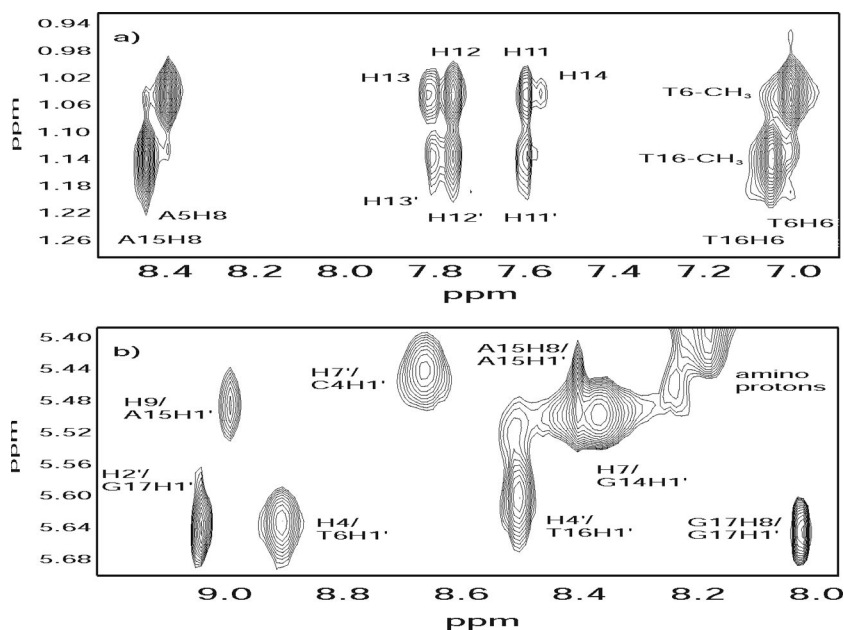


Figure 8. 2D-NOESY spectra of (a) the aromatic/T-Me and (b) the aromatic/sugar H1' regions of the 1:1 reaction mixture of **3** with d(5'-GCGCATCGGC-3') at pH 7.2 and 293 K.

T16 and T6–A15 in the minor groove. The absence of H1'–H8 NOE cross peaks for the nucleotide sequences C7/G8 and C13/G14 could be due to either massive distortion of the double helix or to the presence of a second minor intercalation site between the base pairs C7–G14 and G8–C13. However, no intermolecular NOEs between dppz protons and protons of the base pair G8–C13 are present in the 2D spectrum. Such cross peaks would be expected for dppz intercalation between C7–G14 and G8–C13. The absence of NOE cross peaks to other nucleotides of d(5'-GCGCATCGGC-3') suggests that the bis-intercalation mode of complex **3** is sequence-selective and that other possible binding sites must play, if any, only a minor role.

Both the possible shifts and changes in the exchange kinetics of the hydrogen-bonded nucleobase imino protons on metal complex binding can afford useful insights into the nature of the interaction with the DNA double helix.^[31,32] An upfield shift is characteristic for compounds which intercalate into the duplex and this is observed for all but the resonances of the T6 and T16 imino protons on mixing complex **3** and d(5'-GCGCATCGGC-3') (Figure 9). These broaden considerably at lower metal complex/decanucleotide ratios and then completely disappear at a 1:1 molar ratio, which is in accordance with rapid exchange with the solvent due to interruption of their hydrogen bonds to A15 and A5, respectively. This suggests that the bis-intercalative binding mode of complex **3** must lead to a pronounced distortion of the original B conformation of the duplex, in particular for the base pairs A5–T16 and T6–A15 that are sandwiched between the dppz ligands. The marked broadening of the G imino proton resonances indicates that the metal complex binding causes a significant increase in the base-pair opening rate throughout the whole sequence of the decanucleotide. It is interesting to note that spectrum

(c) in Figure 9 contains two additional imino resonances in comparison to that of the decanucleotide on its own. Although the G17 imino proton could not be assigned with certainty it is probable that it will experience a pronounced upfield shift due to the adjacent intercalating dppz ligand. This suggests that the high field signal at $\delta = 11.40$ ppm may possibly belong to G17. The two additional resonances at $\delta = 12.02$ and 12.13 ppm could be due to the terminal G1 and G11 imino protons, which are not observed for the decanucleotide itself. An alternative explanation would be that they belong to G14 and G17 for a second minor binding mode.

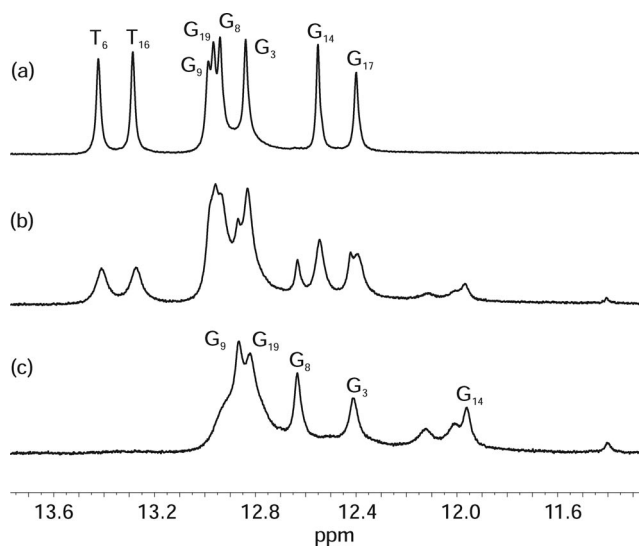


Figure 9. Changes in the imino proton region (11.5–14.0 ppm) of the 1D ^1H NMR spectrum at 293 K of (a) d(5'-GCGCATCGGC-3') upon addition of complex **3** at (b) 0.5:1 and (c) 1:1 molar ratios.

It is interesting to note that, in striking contrast to the present study, extreme broadening of the metal complex ^1H resonances precluded a detailed 2D NMR spectroscopic analysis of the interaction between the complex cation $\Delta\text{[Ru(phen)}_2\text{(dpq)]}^{2+}$ and the dodecanucleotide d(TCGGGATCCCGA)_2 .^[30] This suggests that the metal complex must exchange rapidly between various binding sites. However, the observation of a few relatively strong intermolecular NOEs between the phenanthroline protons and the H4' protons of G3, C8 and C9 did indicate that specific interactions take place in the minor groove. An analysis of the NOESY spectrum of the same Ru complex with the shorter oligonucleotide d(GTCGAC)_2 provided evidence for a preferential intercalation of the dpq ligand from the minor groove between the T2-A5 and C3-G4 base pairs.^[30] The sequence-selective binding in both this case and for the mixture of complex **3** with $\text{d(5'-GCGCATCGGC-3')}$ involves intercalation of the polypyridyl ligand(s) between AT and GC base pairs. It is interesting to note, in this respect, that a sequence-selective intercalation of the dppz ligand between the A5-T2' and C6-G1' base pairs has been reported for the interactions of $[(\eta^5\text{-C}_5\text{Me}_5)\text{Ir(dppz)(H}_2\text{-Met-OMe)}]^{3+}$ and $[(\eta^6\text{-C}_6\text{Me}_6)\text{-Ru(Ac-Met-OH)(dppz)}]^{2+}$ with d(GTCGAC)_2 .^[10,11] NOESY studies with alternative sequences will clearly be necessary to establish whether an A-T base-pair preference or possibly a sequence preference plays an important role in the site-specific binding of complex **3** to oligonucleotide sequences.

The viscosity and ΔT_m data for **1** and **2** (Table 1) suggest that both complexes must also be effective bis-intercalators. Whereas the dithianonane bridging ligand ($n = 5$) will allow two DNA base pairs to be sandwiched by the dppz ligands of complex **2** as for complex **3**, just one base pair can be clamped by the intercalating ligands of **1** due to its shorter dithiaoctane $\text{CH}_3\text{-S-(CH}_2)_n\text{-S-CH}_3$ bridging ligand ($n = 4$). Such a violation of the nearest neighbour exclusion principle has, however, previously been reported for dinuclear platinum complexes of the type $[\{\text{Pt(tpy)}\}_2\{\mu\text{-S-(CH}_2)_n\text{-S}\}]^{2+}$ for $n = 5$ and 6.^[33] The advantageous *cis* position of the Ir-S bonds relative to the dppz ligands enables the $\{(\eta^5\text{-C}_5\text{Me}_5)\text{Ir(dppz)}\}^{2+}$ complexes **2** and **3** to sandwich two rather than one nucleobase pair for the same n values of $n = 5$ and 6.

Conclusions

Organoiridium bis-intercalators can be obtained by linking two $\{(\eta^5\text{-C}_5\text{Me}_5)\text{Ir(dppz)}\}^{2+}$ fragments through a flexible dithiaalkane ligand $\text{CH}_3\text{-S-(CH}_2)_n\text{-S-CH}_3$. UV/Vis and CD spectroscopic studies indicate that adoption of the bis-intercalative binding mode is rapid for complexes **1–3** ($n = 4\text{--}6$) and that the strength of the interaction increases with the value of n within this series. On the basis of an NOESY analysis, complex **3** binds to the decanucleotide d(GCGCATCGGC) from the minor groove between C4 and A5 and T6 and C7 in a sequence-specific manner. The

facile adoption of the bis-intercalating interaction mode and the apparent preference of the $\{(\eta^5\text{-C}_5\text{Me}_5)\text{Ir(dppz)}\}^{2+}$ fragment for A-T base pairs suggests that complexes such as **1–3** offer some potential as sequence-selective DNA binding agents.

Experimental Section

General: UV/Vis spectra were recorded with an Analytik Jena SPECORD 200 spectrometer and CD spectra with a Jasco J-715 instrument in the range 220–300 nm for 1:10 complex/[DNA] mixtures ($[\text{complex}] = 10\text{ }\mu\text{M}$, $[\text{DNA}]$ concentration in $\text{M}(\text{nucleotide}) = 200\text{ }\mu\text{M}$) in a 10 mM phosphate buffer at pH 7.2. LSIMS spectra (LSIMS = liquid secondary ion mass spectrometry) were registered for the mass range $m/z < 3000$ Th with a Fisons VG Autospec employing a caesium ion gun (voltage 17 kV) and 3-nitrobenzyl alcohol as the liquid matrix. Elemental analyses were performed on a Vario EL of Elementar Analysensysteme GmbH. $\text{IrCl}_3\cdot 3\text{H}_2\text{O}$ and $\text{Ag}(\text{CF}_3\text{SO}_3)$ were purchased from Chempur and dithiols and 1,4-dithiane from Aldrich. The starting compound $[(\eta^5\text{-C}_5\text{Me}_5)\text{-IrCl(dppz)}](\text{CF}_3\text{SO}_3)$ and the 2,*n*-dithiaalkanes were prepared in accordance with literature procedures.^[11,34]

4.1 Materials and Methods.

Synthesis of Compounds 1–4

$\{[(\eta^5\text{-C}_5\text{Me}_5)\text{Ir(dppz)}]_2(\mu\text{-2,7-dithiaoctane})\}(\text{CF}_3\text{SO}_3)_4$ (**1**): An equivalent of $\text{Ag}(\text{CF}_3\text{SO}_3)$ (25.7 mg, 0.1 mmol) was added to $[(\eta^5\text{-C}_5\text{Me}_5)\text{IrCl(dppz)}](\text{CF}_3\text{SO}_3)$ (64.5 mg, 0.1 mmol) in 10 mL acetone and stirred in the dark for 0.5 h. Centrifugation of the resulting AgCl precipitate and subsequent solvent removal under vacuum afforded $[(\eta^5\text{-C}_5\text{Me}_5)\text{Ir(acetone)(dppz)}](\text{CF}_3\text{SO}_3)_2$, which was stirred with the ligand 2,7-dithiaoctane (7.5 mg, 0.05 mmol) in $\text{CH}_3\text{OH/CH}_2\text{Cl}_2$ (1:1, 10 mL) at reflux for 48 h. The product was subsequently precipitated with diethyl ether and then repeatedly washed with the same solvent and dried in vacuo. Yield 25% (50 mg). $\text{C}_{66}\text{H}_{64}\text{F}_{12}\text{Ir}_2\text{N}_8\text{O}_{12}\text{S}_6$ (1966.1): calcd. C 40.3, H 3.3, N 5.7, S 9.8; found C 39.9, H 3.4, N 5.3, S 9.7. LSIMS: m/z (%) = 1817 (10) $[\text{M} - \text{OTf}]^+$, 1668 (5) $[\text{M} - \text{OTf} - \text{HOTf}]^+$. ^1H NMR (400 MHz, $[\text{D}_4]\text{MeOH}$, 25 °C): $\delta = 0.91\text{--}1.45$ (m, 8 H, CH_2), 1.60, 1.67 (2s, 6 H, CH_3), 1.73–1.78 (4s, 30 H, $\text{Cp}^*\text{-CH}_3$), 8.20–8.28 (4dd, 4 H, H12/13), 8.36–8.44 (4dd, 4 H, H3/8), 8.51–8.60 (4d, 4 H, H11/14), 9.34, 9.40, 9.47, 9.53 (4d, 4 H, H2/9), 9.81, 9.89, 9.90, 9.92 (4d, 4 H, H4/7) ppm.

$\{[(\eta^5\text{-C}_5\text{Me}_5)\text{Ir(dppz)}]_2(\mu\text{-2,8-dithianonane})\}(\text{CF}_3\text{SO}_3)_4$ (**2**): Preparation as for **1** with the ligand 2,8-dithianonane (8.2 mg, 0.05 mmol). Yield 39% (77 mg). $\text{C}_{67}\text{H}_{66}\text{F}_{12}\text{Ir}_2\text{N}_8\text{O}_{12}\text{S}_6$ (1980.1): calcd. C 40.6, H 3.4, N 5.7, S 9.7; found C 41.0, H 3.4, N 5.5, S 10.0. LSIMS: m/z (%) = 1831 (4) $[\text{M} - \text{OTf}]^+$. ^1H NMR (400 MHz, $[\text{D}_4]\text{MeOH}$, 25 °C): $\delta = 1.08\text{--}1.61$ (m, 10 H, CH_2), 1.58, 1.66 (2s, 6 H, CH_3), 1.73–1.78 (4s, 30 H, $\text{Cp}^*\text{-CH}_3$), 8.20–8.28 (4dd, 4 H, H12/13), 8.36–8.51 (4dd, 4 H, H3/8), 8.53–8.60 (4d, 4 H, H11/14), 9.34, 9.40, 9.47, 9.53 (4d, 4 H, H2/9), 9.80–9.96 (4d, 4 H, H4/7) ppm.

$\{[(\eta^5\text{-C}_5\text{Me}_5)\text{Ir(dppz)}]_2(\mu\text{-2,9-dithiadecane})\}(\text{CF}_3\text{SO}_3)_4$ (**3**): Preparation as for **1** with the ligand 2,9-dithiadecane (8.9 mg, 0.05 mmol). Yield 20% (40 mg). $\text{C}_{68}\text{H}_{68}\text{F}_{12}\text{Ir}_2\text{N}_8\text{O}_{12}\text{S}_6$ (1994.1): calcd. C 41.0, H 3.4, N 5.6, S 9.6; found C 41.4, H 3.0, N 5.5, S 9.4. LSIMS: m/z (%) = 1845 (8) $[\text{M} - \text{OTf}]^+$. ^1H NMR (400 MHz, $[\text{D}_4]\text{MeOH}$, 25 °C): $\delta = 0.89\text{--}1.45$ (m, 12 H, CH_2), 1.60, 1.67 (2s, 6 H, CH_3), 1.73–1.78 (4s, 30 H, $\text{Cp}^*\text{-CH}_3$), 8.20–8.28 (4dd, 4 H, H12/13), 8.36–8.44 (4dd, 4 H, H3/8), 8.51–8.60 (4d, 4 H, H11/14), 9.34, 9.40, 9.47, 9.53 (4d, 4 H, H2/9), 9.81, 9.89, 9.92, 9.95 (4d, 4 H, H4/7) ppm.

[$\{\eta^5\text{-C}_5\text{Me}_5\text{Ir}(\text{dppz})\}_2(\mu\text{-1,4-dithiane})\}(\text{CF}_3\text{SO}_3)_4$ (4**):** Preparation as for **1** with the ligand 1,4-dithiane (6.0 mg, 0.05 mmol). Yield 45% (87 mg). $\text{C}_{64}\text{H}_{58}\text{F}_{12}\text{Ir}_2\text{N}_8\text{O}_{12}\text{S}_6$ (1936.0): calcd. C 39.7, H 3.0, N 5.8; found C 39.7, H 2.8, N 5.6. LSIMS: m/z (%) = 1935 (3) $[\text{M} - \text{OTf}]^+$. ^1H NMR (400 MHz, $[\text{D}_4]\text{MeOH}$, 25 °C): δ = 1.08–1.61 (m, 8 H, CH_2), 1.58, 1.66 (2s, 6 H, CH_3), 1.73–1.78 (4s, 30 H, $\text{Cp}^*\text{-CH}_3$), 8.16–8.23 (m, 4 H, H12/13), 8.38–8.52 (4dd, 4 H, H3/8), 8.55–8.60 (4d, 4 H, H11/14), 9.37, 9.43, 9.65, 9.71 (4d, 4 H, H2/9), 9.94, 10.04, 10.08, 10.12 (4d, 4 H, H4/7) ppm.

X-ray Structural Analysis of 4: Crystals of **4** suitable for X-ray structural analysis were grown by slow evaporation of a $\text{CH}_3\text{OH}/\text{H}_2\text{O}$ solution. $[\text{C}_{60}\text{H}_{58}\text{Ir}_2\text{N}_8\text{S}_2] \cdot 12[\text{CF}_3\text{O}_3\text{S}] \cdot 8\text{H}_2\text{O}$, $M = 5952.0$, triclinic, space group $P\bar{1}$ (no. 2), $a = 14.188(6)$, $b = 18.332(8)$, $c = 23.738(10)$ Å, $\alpha = 99.969(9)$, $\beta = 101.724(8)$, $\gamma = 107.624(9)^\circ$, $V = 5577(4)$ Å³, $D_{\text{calcd.}} = 1.772$ Mg m⁻³, μ (Mo- K_α) = 3.84 mm⁻¹; data collection with a Bruker axs CCD diffractometer using 1° ω scans in the range $\theta \leq 27.7^\circ$ with graphite-monochromated Mo- K_α radiation ($\lambda = 0.71073$ Å). The intensity data were corrected empirically for absorption ($T_{\text{min}} = 0.531$, $T_{\text{max}} = 0.630$) and the structure was solved by direct methods with SHELXS97 and refined against F_o^2 using SHELXL97.^[35] Anisotropic temperature factors were employed for non-hydrogen atoms and cation protons were included at geometrically calculated positions as riding atoms. The final R factors were $R_1 = 0.057$ for 18078 reflections with $I > 2\sigma(I)$ and $wR_2 = 0.157$, $S = 1.03$ for all 24712 independent reflections.

CCDC-755134 contains the supplementary crystallographic data for compound **4**. These data can be obtained free of charge from the Cambridge Crystallographic Data Centre via www.ccdc.cam.ac.uk/data_request/cif.

Electronic Spectra and DNA Binding Studies: UV/Vis spectra were recorded over a period of 48 h for 1:10 complex/[DNA] mixtures [complex = 10 μM , DNA concentration in M(base pairs) = 100 μM] in a 10 mM phosphate buffer (pH 7.2) with an Analytik Jena SPECORD 200 spectrometer. To assure solubility of the complexes, 1% DMSO was added to all of the aqueous buffer solutions. Thermal denaturation temperatures T_m of 1:20 complex/[DNA] mixtures were measured by recording melting curves at 1 °C steps for the wavelength 260 nm on the SPECORD 200 spectrometer equipped with a Peltier temperature controller. T_m values were calculated by determining the midpoints for melting curves from first-order derivatives and are estimated to be accurate within 1 °C. Concentrations of CT DNA were determined spectrophotometrically using the molar extinction coefficient $\epsilon_{260} = 13200 \text{ M}^{-1} \text{ cm}^{-1}$.^[36]

Viscosity Measurements: Viscosities for sonicated DNA alone and for complex/sonicated DNA mixtures were determined using a Cannon-Ubbelohde Semi-micro dilution viscometer (Series No. 75, Cannon Instrument Co) held at 25 °C. The measurements were performed for a 0.4 mM DNA solution in a phosphate buffer (10 mM, pH = 7.2) and for complex (0.4 mM)/DNA(0.4 mM) mixtures. Reduced viscosities η_0 for DNA alone and η for the complex/DNA mixtures at $r = 0.1$ were calculated by the literature method.^[27] These were converted into the function $(L - L_0)/(L_0 \cdot r)$ using the relationship $(\eta/\eta_0)^{1/3} = (L/L_0)$, where L is the DNA length in a complex/DNA mixture and L_0 is the length of DNA alone.^[27] Ethidium bromide was employed as a standard intercalator to confirm the experimental conditions and gave a value of $(L - L_0)/(L_0 \cdot r) = 0.97$ for an ethidium bromide/DNA mixture at $r = 0.1$.

NMR Spectroscopy: A Bruker DRX 400 spectrometer was employed for the registration of ^1H NMR spectra with chemical shifts being reported as δ values relative to the signal of the deuterated solvent. The splittings of proton resonances in the reported 1D ^1H NMR spectra are defined as s = singlet, d = doublet, t = triplet

and m = multiplet. The decanucleotide spectra with WATERGATE solvent suppression were recorded at 600.13 MHz proton frequency and at 293 K on a Bruker DRX 600 spectrometer equipped with a pulsed field gradient and a triple resonance probehead.^[37–39] The 1D ^1H NMR spectra were recorded with a time domain of 32 k data points and a spectral width of 12019.23 Hz. The sweep width of the 2D homonuclear spectra was 12019.23 Hz in the direct and in the indirect ^1H dimension. The free-induction decay was acquired for 340.9 ms and the dwell time was set to 41.6 μs . Homonuclear and NOESY spectra were zero-filled prior to Fourier transformation and sine apodisation functions were applied in both dimensions. Assignments were obtained from 2D COSY, TOCSY and NOESY using previously published procedures.^[40–46] All spectra were processed with NMR-Pipe and analysed with NMRView.^[47,48] Assignment and data handling were performed using NMRView.^[48]

Acknowledgments

We are grateful to Heike Mayer-Figge for excellent technical assistance and to the Deutsche Forschungsgemeinschaft (DFG) for financial support of this work within the research group FOR 630 “Biological function of organometallic compounds”.

- [1] K. E. Erkkila, D. T. Odom, J. K. Barton, *Chem. Rev.* **1999**, 99, 2777–2795.
- [2] C. Metcalfe, J. A. Thomas, *Chem. Soc. Rev.* **2003**, 32, 215–224.
- [3] N. J. Wheate, C. R. Brodie, J. G. Collins, S. Kemp, J. R. Aldrich-Wright, *Mini-Rev. Med. Chem.* **2007**, 7, 627–648.
- [4] A. E. Friedman, J. C. Chambron, J. P. Sauvage, N. J. Turro, J. K. Barton, *J. Am. Chem. Soc.* **1990**, 112, 4960–4962.
- [5] D. M. Fisher, P. J. Bednarski, R. Grunert, P. Turner, R. R. Fenton, J. R. Aldrich-Wright, *ChemMedChem* **2007**, 2, 488–495.
- [6] E. L. Menon, R. Perera, M. Navarro, R. J. Kuhn, H. Morrison, *Inorg. Chem.* **2004**, 43, 5373–5381.
- [7] S. Schäfer, W. S. Sheldrick, *J. Organomet. Chem.* **2007**, 692, 1300–1309.
- [8] S. Schäfer, I. Ott, R. Gust, W. S. Sheldrick, *Eur. J. Inorg. Chem.* **2007**, 3034–3046.
- [9] M. Scharwitz, I. Ott, Y. Geldmacher, R. Gust, W. S. Sheldrick, *J. Organomet. Chem.* **2008**, 693, 2299–2309.
- [10] A. Frodl, D. Herebian, W. S. Sheldrick, *J. Chem. Soc., Dalton Trans.* **2002**, 3664–3673.
- [11] D. Herebian, W. S. Sheldrick, *J. Chem. Soc., Dalton Trans.* **2002**, 966–974.
- [12] R. Stodt, S. Gencaslan, A. Frodl, C. Schmidt, W. S. Sheldrick, *Inorg. Chim. Acta* **2003**, 355, 242–253.
- [13] C. Metcalfe, M. Webb, J. A. Thomas, *Chem. Commun.* **2002**, 2026–2027.
- [14] C. Metcalfe, I. Haq, J. A. Thomas, *Inorg. Chem.* **2004**, 43, 317–323.
- [15] S. P. Foxon, T. Phillips, M. R. Gill, M. Tourie, A. W. Parker, M. Webb, J. A. Thomas, *Angew. Chem. Int. Ed.* **2007**, 46, 3680–3688.
- [16] B. Önfelt, P. Lincoln, B. Nordén, *J. Am. Chem. Soc.* **1999**, 121, 10846–10847.
- [17] B. Önfelt, P. Lincoln, B. Nordén, *J. Am. Chem. Soc.* **2001**, 123, 3630–3637.
- [18] M. Hogan, N. Dattagupta, D. M. Crothers, *Biochemistry* **1979**, 18, 280–288.
- [19] M. F. Brana, M. Cacho, A. Gradillas, B. Pascual-Teresa, A. Ramas, *Curr. Pharm. Des.* **2001**, 7, 1745–1780.
- [20] L. D. Van Vliet, T. Ellis, P. J. Foley, L. Liu, F. M. Pfeffer, R. A. Russell, R. N. Warren, F. Holfelder, M. J. Waring, *J. Med. Chem.* **2007**, 50, 2326–2340.
- [21] P. J. Bond, R. Langridge, K. W. Jennette, S. J. Lippard, *Proc. Natl. Acad. Sci. USA* **1975**, 72, 4825–4829.
- [22] *Hyperchem(TM)*, Hypercube Inc., Gainesville, Florida, USA.

- [23] S. Gencaslan, W. S. Sheldrick, *Eur. J. Inorg. Chem.* **2005**, 3840–3849.
- [24] V. Brabec, V. Kleinwächter, J.-L. Butour, N. P. Johnson, *Biophys. Chem.* **1990**, 35, 129–141.
- [25] D. M. Gray, in: *Circular Dichroism and the Conformational Analysis of Biomolecules* (Ed.: G. D. Fasman), Plenum Press, New York, **1996**, p. 469–500.
- [26] W. C. Johnson, in: *Circular Dichroism: Principles and Applications*, 2nd edition (Eds.: N. Berova, K. Nakanishi, R. W. Woody), VCH Publishers, New York, **2000**, p. 523–540.
- [27] C. Cohen, H. Eisenberg, *Biopolymers* **1966**, 4, 429–440.
- [28] D. Suh, J. B. Chaires, *Bioorg. Med. Chem.* **1995**, 3, 723–728.
- [29] C. M. Dupureur, J. K. Barton, *J. Am. Chem. Soc.* **1994**, 116, 10286–10287.
- [30] J. G. Collins, A. D. Steedmann, J. R. Aldrich-Wright, I. Greguric, T. W. Hambley, *Inorg. Chem.* **1998**, 37, 3133–3141.
- [31] J. Feigon, W. A. Denny, W. Leupin, D. R. Kearns, *J. Med. Chem.* **1984**, 27, 450–465.
- [32] M. Kochoyan, J. L. Leroy, M. Gueron, *J. Mol. Biol.* **1987**, 196, 599–609.
- [33] W. D. McFadyen, L. P. G. Wakelin, I. A. G. Roos, B. L. Hillcoat, *Biochem. J.* **1986**, 238, 757–763.
- [34] E. Anklam, *J. Photochem. Photobiol. A: Chem.* **1989**, 46, 77–86.
- [35] G. M. Sheldrick, *SHELXS97 and SHELXL97*, Göttingen, Germany, **1997**.
- [36] J. Marmur, *J. Mol. Biol.* **1961**, 3, 208–218.
- [37] L. Braunschweiler, R. R. Ernst, *J. Magn. Reson.* **1983**, 53, 521–528.
- [38] D. G. Davis, A. Bax, *J. Am. Chem. Soc.* **1985**, 107, 7197–7198.
- [39] A. J. Shaka, C. J. Lee, A. Pines, *J. Magn. Reson.* **1988**, 77, 274–293.
- [40] A. Bax, D. G. Davis, S. K. Sarkar, *J. Magn. Reson.* **1985**, 63, 230–234.
- [41] J. K. Song, J. L. Marklex, *J. Mol. Recognit.* **2001**, 14, 166–171.
- [42] V. Sklenar, M. Piotto, R. Leppik, V. Saudek, *J. Magn. Reson., Ser. A* **1993**, 102, 241–245.
- [43] R. Stoll, C. Renner, S. Hansen, S. Palme, C. Klein, A. Belling, W. Zeslawski, M. Kamionka, T. Rehm, P. Muhlhahn, R. Schuhmacher, F. Hesse, B. Kaluza, W. Voelter, R. A. Ergh, T. A. Holak, *Biochemistry* **2001**, 40, 336–344.
- [44] R. Stoll, C. Renner, M. Zweckstetter, M. Bruggert, D. Ambrosius, S. Palme, R. A. Enrgh, M. Golob, I. Breibach, R. Buettner, W. Voelter, T. A. Holak, A. K. Broscherhoff, *EMBO J.* **2001**, 20, 340–349.
- [45] A. Derome, M. Williamson, *J. Magn. Reson.* **1990**, 88, 177–185.
- [46] M. Piotto, V. Sandek, V. Sklenar, *J. Biomol. NMR* **1992**, 2, 661–666.
- [47] F. Delaglio, S. Grzesiek, G. W. Vuister, G. Zhu, J. Pfeifer, A. Bax, *J. Biomol. NMR* **1995**, 6, 277–293.
- [48] R. D. Johnson, P. Bluemler, R. Rafey, D. Brodbeck, *Abstr. Papers Am. Chem. Soc.* **1994**, 207, 138–COMP.

Received: November 19, 2009

Published Online: February 25, 2010